Sandwave migration predictor based on shape information

M. A. F. Knaapen

Department of Water Engineering and Management, University of Twente, Enschede, Netherlands

Received 24 June 2004; revised 11 February 2005; accepted 21 February 2005; published 4 October 2005.

[1] Migration of offshore seabed waves, which endangers the stability of pipelines and communication cables, is hard to measure. The migration rates are small compared to the measurement errors. Here, sandwave migration rates are determined from the change in the crest position deduced from long time series of bathymetric echo-sounding data. The crests are identified as local extremes in a bathymetric profile, after low-pass filtering. This approach is applied to both two-dimensional data and to profiles along pipelines. A consistent migration rate of several meters per year is found. A strong correlation between the sandwave shape and the migration rate is translated in a migration predictor. The predictor assumes that the sandwaves migrate in the direction of the steepest slope, following a quadratic relation with the asymmetry. Furthermore, it is included that longer waves travel faster but higher waves travel slower. The predictor is calibrated against data from nine areas and validated using three additional areas. An error analysis using markers shows that the error of the predictor is small compared to the noise in the individual crest position observations.

Citation: Knaapen, M. A. F. (2005), Sandwave migration predictor based on shape information, *J. Geophys. Res.*, *110*, F04S11, doi:10.1029/2004JF000195.

1. Introduction

[2] Sandy shallow seas, like the Bisanseto Sea in Japan, the continental shelf between the Indonesian archipelago and the North Sea, are intensively used. Many of the world's important harbors are situated near sandy shelf seas. Furthermore, pipelines transporting gas and oil and communication cables cross the seas. Therefore it is important to understand the dynamics of the sandy beds of these shelf seas. In general the sandy shallow seas are situated in regions with fairly mild conditions in which sand is transported without being flushed away immediately. The interaction between these conditions and the seabed results in a wide range of bed patterns (Table 1).

[3] From these patterns, the sandwaves are of special interest to human activity. They cover large parts of the sandy beds of shallow seas, can reduce the depth considerably [*Katoh et al.*, 1998] and are known to migrate. As they are more dynamic than the larger sand ridges and sandbanks, they endanger both shipping and the pipeline and cables in the shelf seas (Figure 1). The migration of the sandwaves may expose pipelines and cables, sometimes even resulting in free spans [*Morelissen et al.*, 2003]. The long-term migration of the sandwaves can be caused by residual currents [*Németh et al.*, 2002] and by tidal asymmetry due to higher components [*Besio et al.*, 2004]. Although this migration can be modeled, it is difficult to estimate the migration rates. The models are idealized and depend on parameters and input that are difficult or impossible to measure or estimate theoretically, e.g., turbulent viscosity, bed friction and the residual current.

0148-0227/05/2004JF000195

[4] Another problem is the lack of accurate observations of migrating sandwaves. Publications on observed migration are scares and in most cases the observed displacement hardly exceeds the accuracy of the positioning system that has been used. For this reason, there has been an ongoing discussion on sandwave migration going back to *Terwindt* [1971]. For example, *Lanckneus and De Moor* [1995] show results of small displacements of a few meters within a year, with some occurrences. However, as all displacements are within the error margin of the positional error, they conclude that no net movement can be inferred from these data. *Katoh et al.* [1998] describe migration of sandwaves on top of a shoal. However, clear rates have not been determined. Moreover, the observations result from monitoring after dredging. It is difficult to determine whether this migration is true migration or the result from the reformation after the dredging. *Idier et al.* [2002] observe clear migration of 9–17 m/yr of an individual sandwave in the English Channel between 1999 and 2001. *Morelissen et al.* [2003] describe the migration of a few sandwaves along two sections of a pipeline in the North Sea of 10 and 20 m/yr in the assumed direction of the residual current and *Besio et al.* [2004] find a migration of 3 m per year against the assumed residual current along a pipeline in front of the Belgian coast.

[5] In all cases the migration has been determined using a visual interpretation of individual profiles. A determination of the accuracy of the available data is missing in all cases, but based on the description of the interpretations, the measurement errors in the data will be significant.

[6] This paper presents an approach to objectively analyze large number of sandwaves on their migration. The migration is determined for nine areas on the Dutch Con-

Table 1. Orders of Magnitude of the Characteristics of Offshore Sand Bed Forms: Wavelength L, Height H, the Migration Rate c, and the Typical Timescale T in Which the Patterns Evolve Following the Definitions of *Reineck et al.* [1971][a]

Bed Form	*Ashley* [1990]	L, m	H, m	T	c, m/y
Ripples	ripples	1	0.01	hours	1000
Megaripples	medium to large dunes	10	0.1	days	100
Sandwaves	very large dunes	200	5	years	10
Long bed waves[b]	?	1500	5	unknown	unknown
Shoreface connected ridges	ridges	4000	5	centuries	1
Tidal sandbanks	ridges	6000	10	centuries	1

[a]Each pattern is related to a distinct flow mechanism. For completeness, the terminology of *Ashley* [1990], which is generally accepted among geologists, is given as well. For an overview on the literature of these patters, see, e.g., *Dodd et al.* [2003].
[b]For an explanation of this pattern, see *Knaapen et al.* [2001].

tinental Shelf using this approach. The accuracy of this approach and the available data are analyzed thoroughly for two echo-sounding data sets; one profile along a pipeline, and one multibeam data set.

[7] For practical purposes it is a drawback, if one needs long time series of observation to determine the migration rate. Therefore a migration predictor is proposed based on the median shape characteristics of the sandwaves in section. With such a predictor the migration rate can be estimated without the availability of bathymetric time series superfluous.

[8] This approach seems to disagree with the observation on the Middelkerke sand bank [*Lanckneus and De Moor*, 1994, 1995], that sandwaves can change their orientation on a seasonal timescale, without showing significant migration of the sandwaves. This would imply that our predictor could predict migration, whereas the observations show stationary sandwaves. However, a short discussion will show otherwise.

[9] The outline of this paper is as follows. First the available data is presented in section 2. Next, the data analysis is explained in section 3. The results of this analysis are presented in section 4. In section 5 the migration predictor is derived, calibrated and validated. The accuracy of the results is determined in section 6. We end with a discussion on the predictor in section 7 and the conclusions in section 8.

2. Available Bathymetric Data

[10] We will estimate and predict sandwave migration from bathymetric data in twelve areas throughout the Southern Bight of the North Sea and the English Channel. The metadata of these areas are summarized in Table 2. In the area, the tide is fairly one dimensional with the flow from north to south and vice versa. Figure 2 shows tidal ellipses as modeled by *McCave* [1971] near the bottom. The depth-averaged tidal velocity amplitude, averaged over a spring neap cycle, is about 0.7 m/s. There is a small residual current in north-northeasterly direction with a velocity in the order of 0.1 m/s [*McCave*, 1971; *Otto et al.*, 1990]. Figure 2 shows the position within the North Sea of the nine areas. The three pipeline data are being used under a confidentiality agreement, so their location cannot be revealed.

2.1. Multibeam Profiles

[11] From the available multibeam bathymetric data 7 rectangular areas are selected. These areas are defined such that one of the axes is parallel to the direction of the principal tidal axis. As an example, Figure 3 gives the resulting bathymetry for the Ectomorph area. Consequently, this axis is perpendicular to the direction of the sandwave crests. The data are provided by the North Sea Directorate of the Netherlands Ministry of transport, Public Works and Water Management, and result partly from their routine surveys and partly from the Delft Cluster project "Ecomorphodynamics of the Sea Bed" [*Baptist et al.*, 2001; *Weber et al.*, 2004]. In general, the surveys have a resolution of one observation per square meter, but a detail of the Ecomorphodynamics area has been surveyed with a resolution of nine observations per square meter. The latter surveys will be used to analyze the accuracy of the data.

2.2. Single-Beam Profiles Along Pipelines

[12] The pipeline data set contain 5 surveys taken along two pipelines, both covering about 9 km (Figure 4). The surveys cover the period between 1995 and 2000. The data were gathered by digitizing profile maps from the Netherlands State Supervision of Mines. Although this digitization introduces additional noise, the data is still reliable enough to analyze the sandwave migration. The pipelines 1 and 2 are almost parallel to the principal tidal direction, and thus perpendicular to the sandwave crests. This is confirmed by the contour lines on the maps. For pipeline 3, the contour lines on the maps show that there is an 45° angle between the sandwave cress and the pipeline. Therefore all length estimates are corrected for this angle. The surveys cover about 30 (pipelines 1 and 2) and 55 sandwaves (pipeline 3).

3. Data Analysis

[13] The classical approach to analyze rhythmic bed patterns has been to determine the locations of the crest

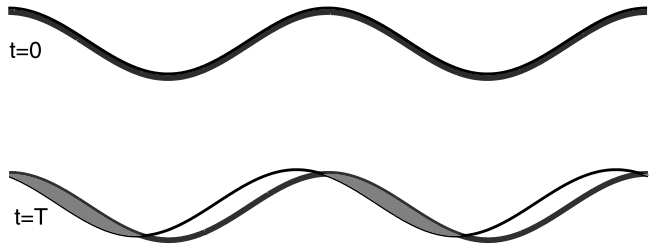

Figure 1. Pipeline exposure due to sandwave migration. The pipeline (bold line) is exposed as the sandwave (thin line) migrates between (top) $t = 0$ and (bottom) $t = T$. The shading shows areas of exposure.

Table 2. Metadata for the 12 Bathymetric Survey Series

Area	Easting, m[a]	Northing, m[a]	Length, m	Width, m	Period	Number[b]
			Calibration			
Twin	459510	5722070	4250	2350	1996–2002	5
NH 1[c]	483950	5747950	5000	2000	1997–2002	4
NH 2[c]	491020	5755020	5000	2000	1997–2002	4
Short stay	494950	5754950	5000	2000	1995–2002	6
ACh. 1[c]	499950	5756450	5000	2000	1995–2002	6
ACh. 2[c]	509950	5760950	2500	4000	1995–2002	6
Ecomorph	561420	5836210	5000	1000	2001–2003	4
Pipeline 1[d]	conf.	conf.	9000	0	1995–2000	5
Pipeline 2[d]	conf.	conf.	9000	0	1995–2000	5
			Validation			
Deep water region	410750	5674500	10000	1000	1995–2003	9
Thames Estuary	405000	5740500	1800	2000	1995–2003	9
Pipeline 3[d]	conf.	conf.	30000	0	1997–2003	14

[a]Coordinates of the center points in UTM.
[b]Number of surveys used.
[c]From the North Hinder region (NH) and the Approach Channel region (ACh), two areas are selected.
[d]The pipeline data are used under a confidentiality agreement. All three pipes are in the north of the Southern Bight.

and trough. These positions are then compared to determine the length, height and other characteristics [*O'Conner*, 1992]. This approach has been proven to be robust and reliable. This approach can easily be used to estimate migration as well. An automated procedure has been created to determine the crest and trough positions in both one-dimensional and two-dimensional bathymetric data. For this purpose the data is filtered using a low-pass filter. The choice of the specific window has little to no effect on the results. The low-pass filter removes all noise related to megaripples and ripples, i.e., all signals with a wavelength shorter than 30 m. The crests and troughs can than be identified as the local maxima and minima of the bed levels in the direction of the principle tidal axis, respectively. The level of these minima and maxima are then retrieved from the raw, unfiltered data set. This avoids a underprediction of the sandwave heights due to the filtering procedure. Instead the error is equal to the noise of the superimposed small-scale bed patterns. Figure 5 gives the resulting positions for the multibeam data set.

[14] The shape characteristics of the sandwaves can be deduced from the crest and trough positions of a single survey (Figure 6). The length of a sandwave is defined as the distance between the trough positions on opposite sites of the crest:

$$L = |x_2 - x_1|. \tag{1}$$

The asymmetry is characterized as the difference of the distance between the trough north of the crest and the distance between the crest and the trough south of the crest divided by the sandwave length:

$$A = \frac{L_2 - L_1}{L} = \frac{|x_2 - x_{\text{crest}}| - |x_{\text{crest}} - x_1|}{L}. \tag{2}$$

Finally, the height is defined as the difference between the crest level and the baseline of the two trough levels:

$$H = z_{\text{crest}} - \frac{z_1 L_2 + z_2 L_1}{L}. \tag{3}$$

If the crests and trough positions have been determined for all surveys, the nett displacement of these positions can be used to estimate the migration rate. Using the knowledge

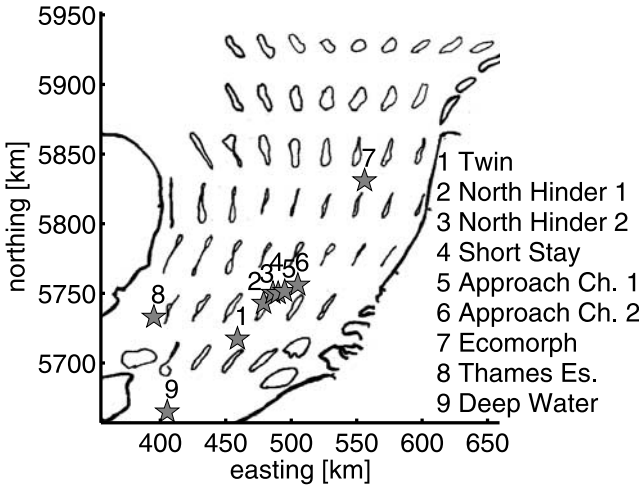

Figure 2. Location of the research areas together with the calculated ellipses according to *McCave* [1971]. On the left, parts of East Anglia and Kent in the United Kingdom are visible, and Belgium and the Netherlands can be recognized on the right of the figure.

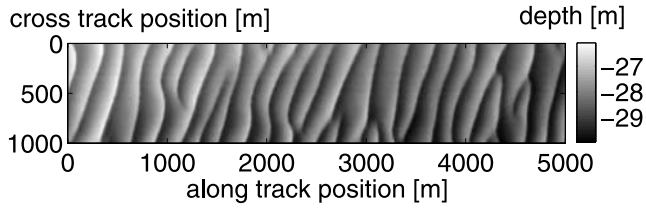

Figure 3. Bathymetric map of the sandwave area Ecomorph in 2001. The principal tidal direction is from left to right, with right being N-NE. The bed level is given relative to mean sea level.

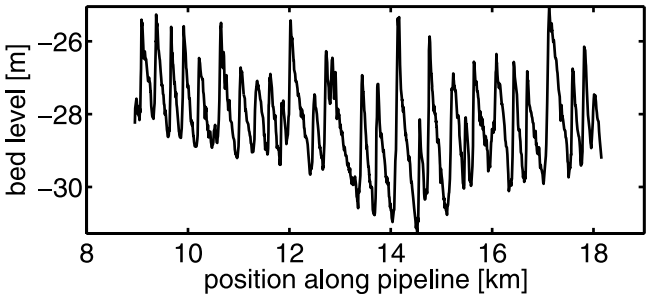

Figure 4. Bathymetric profile along the pipeline, situated parallel to the principal tidal current direction. The assumed residual current is from right to left, with left being N-NE. The bed level is given relative to mean sea level.

from literature [*Idier et al.*, 2002; *Morelissen et al.*, 2003; *Németh et al.*, 2002; *Besio et al.*, 2004] that the migration rates are small compared to the wavelength, the crest and trough positions of two consecutive surveys are compared. All crests (troughs) in one of the surveys that are close to a crest (trough) position in the other survey (i.e., the cross track position is the same and the difference in the along track is less than a predefined limit, here being 50 m, 25% of the wavelength) are used. The positions that do not have a match in the other survey are removed. Now, the difference between the coupled crest (trough) positions gives the migration in the period between the surveys. This results in estimates of the migration of all crests.

[15] In this paper the approach is used to estimate sandwave characteristics. Since it is independent of length scales or hydraulic conditions, it can easily be adapted for the analysis of other rhythmic patters, like tidal sand banks, megaripples or ripples in coastal seas or similar patterns in rivers.

4. Observed Sandwave Migration

[16] For every area, the crest and trough positions during the survey period are compared. The first survey is used to determine the representative sandwave shape. In general the statistics of the results are non-Gaussian. The singularities in the sandwave patterns, e.g., the bifurcations, result in an fairly large number of short an low waves and a small number of very long waves. Figure 7 gives the results for the Ectomorph area, which has a fairly regular sandwave pattern. Other areas give more disrupted distributions. Therefore the median values of the different shape characteristics are chosen as being representative for the sandwaves in the area. Table 3 summarizes the resulting sandwave characteristics.

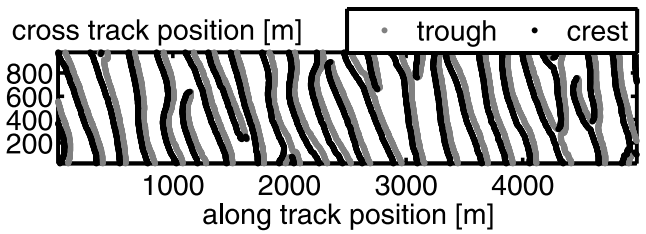

Figure 5. Crests and troughs of the sandwaves in the Ectomorph area in 2001. The principal tidal direction is from left to right, with right being northeast.

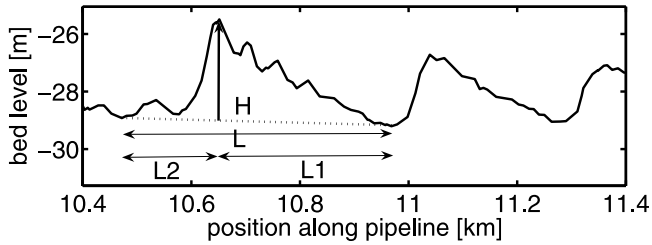

Figure 6. Definition of the sandwave characteristics.

[17] Using the crest positions in the first survey as the zero position, the spatial average displacement of the crest positions is determined for each survey. This average value is a valid approximation, as the distribution of the displacements is almost Gaussian. As an indication of the variation in the values, the standard deviation is determined as well. A linear trend analysis is applied on the resulting displacements in time to estimate the time averaged migration rate. Figure 8 shows the results for the Twin area. Table 3 gives the estimated migration rates for all areas. In general the sandwave migration rate is small. Only in the Pipeline data and the Ectomorph area, which are all situated in the northern part of the Southern Bight, the migration rates exceed 1 m/yr. All sandwaves migrate to the north except for the ones in the Twin area.

5. Predicting Migration

[18] The migration rates have been determined for the nine areas for which bathymetric time series are available. In general these rates are based on time series over periods of several years. Only using markers, shorter time series are useful. In this section we present a migration predictor based on shape characteristics. Of the available data sets, 9 will be used to calibrate the predictor. The remaining three areas, deep water, Thames Estuary and pipeline 3, are used to validate the predictor.

5.1. Deduction of the Migration Predictor

[19] In practice, it is generally accepted that lee-stoss asymmetry of bed forms is a sign for bed form migration in the direction of the steeper slope. This assumption is

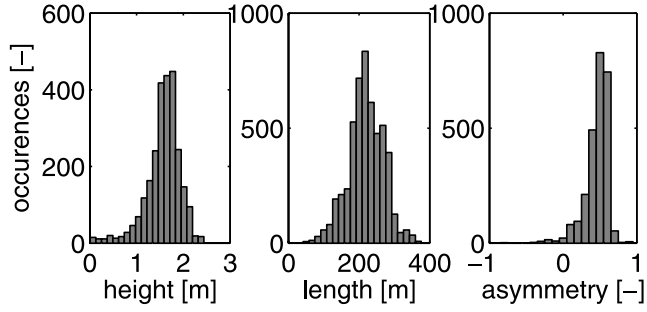

Figure 7. Histograms showing distribution of the sandwave characteristics in the Ectomorph area. Note the long tails in both the asymmetry and height distributions, which are even more apparent in the other areas.

Table 3. Sandwave Characteristics (Length L, Height H, Asymmetry A_s, Migration Rate c, and Angle) for the Nine Bathymetric Survey Series

Area	L, m	H, m	A_s	c, my^{-1}	Angle,[a] deg
Twin	164.5	1.5	−0.14	−0.6	35
North Hinder 1	254.6	1.9	0.03	−0.2	45
North Hinder 2	224.5	2.4	0.03	−0.2	45
Short stay	235.5	2.2	0.11	0.1	45
Approach Ch. 1	230.3	2.5	0.14	0.2	45
Approach Ch. 2	244.2	2.2	0.10	0.3	45
Ectomorph	217.4	1.6	0.47	6.1	15
Pipeline 1	323.4	2.5	0.44	8.4	···
Pipeline 2	340	3.4	0.40	4.4	···
Deep water region	211.0	1.46	0.00	0.1	25
Thames Estuary	110.6	0.7	0.06	0.2	20
Pipeline 3	273.60	1.53	0.22	2.9	···

[a]The angle is the migration direction relative to the north.

confirmed by the work of *Németh et al.* [2002]. They show that tidal asymmetry not only results in migration of sandwaves, but also in lee-stoss asymmetry. The migration is indeed in the direction of the steeper slope. This relation is confirmed by the data in Table 3. Figure 9 shows a clear relation between the migration rate and the lee-stoss asymmetry. The migration seems to be related to some power of the asymmetry and the sign of the migration agrees with the sign of the lee-stoss asymmetry.

[20] Another assumption from the field is that bigger bed forms move slower. In the extreme this is clear as ripples move faster than megaripples that again move faster than sandwaves. Using scientific intuition, this makes sense as well for the sandwave height. With equal wavelength, more sediment transport is required to move a high sandwave than to move a low sandwave. At first sight, however, such a relation is not clear from the data in Table 3. Nevertheless, we will use this assumption for our migration predictor.

[21] It is unclear how the wavelength influences the migration rate. Similar to the argumentation about the height, one could say that longer waves require more sediment transport. However, now this increased sediment transport can be divided over a larger surface length. The sediment transport unit length remains constant. The impact of the wavelength cannot be deduced easily, but Table 3 shows than the correlation between the wavelength is stronger that the correlation with the inverse of the wavelength. Therefore we assume a positive correlation between the wavelength and the migration rate.

[22] On the basis of the above relations, it makes sense to look for a predictor based on the product of the length-to-height ration (L/H) and a power of the asymmetry (A). Using a trial and error approach, several parameter combinations have been tried, with varying success. Table 4 summarizes the found value of fitness for these parameter combinations to predict the sandwave migration. The relationship between the migration and the asymmetry is much stronger than the relation with the wavelength and the height. A linear function of the asymmetry gives a lower value than some power of the asymmetry. The squared value ($|A|A$) gives the best fit, but the third power gives reliable predictions as well.

[23] Intriguing is the effect of the wavelength and the ratio $\frac{L}{H}$. Individually, these elements do not contribute to the accuracy of the predictor, but their product $L\frac{L}{H}$ improves the predictor considerably. This suggests that the combination is indeed an important factor in the migration predictor.

[24] Combining the information on the correlation results in a migration predictor of the following shape:

$$c = \alpha L \frac{L}{H} A|A|, \tag{4}$$

in which α is the calibration constant with dimension y^{-1}.

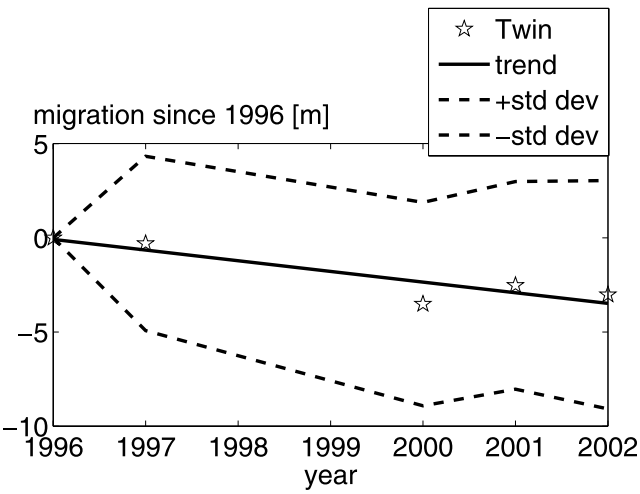

Figure 8. Sandwave migration in the Twin area. The dots give the observed displacements relative to the 1996 survey. The migration rate is determined using a linear trend (bold line). The thin lines give the confidence interval defined by the standard deviation.

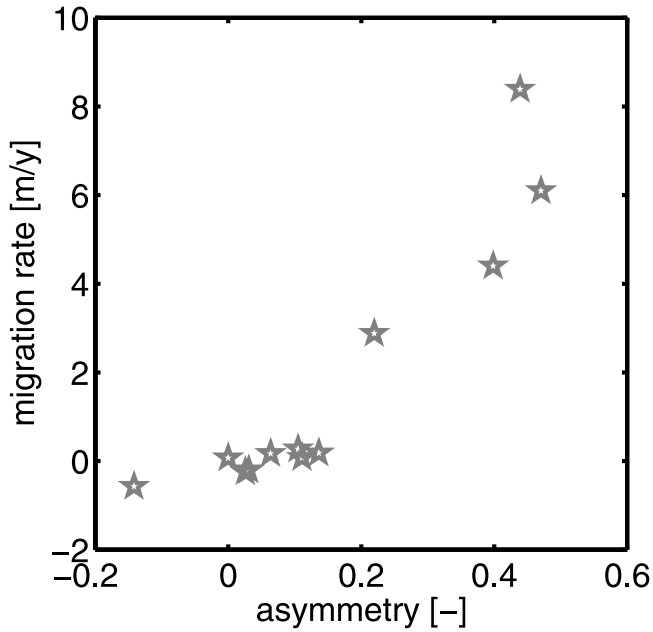

Figure 9. Clear relation between the migration rate and the asymmetry of the sandwaves in the nine selected areas.

Table 4. Measure of Fitness to Predict Sandwave Migration for Several Parameters

Parameter	L/H	$1/L$	L	A_s	$A_s\ L$	A_s^2	$A_s^2\ L$	$A_s^2(L/H)$	$A_s^2\ L(L/H)$	$A_s^3\ L(L/H)$
R^2	0.06	0.19	0.28	0.83	0.84	0.92	0.93	0.92	0.98	0.97

5.2. Calibration and Validation

[25] The calibration of the predictor against the observations in nine out of twelve areas resulted in

$$c = 2.2 \cdot 10^{-7} n\sigma L \frac{L}{H} A|A| = 9.78 \cdot 10^{-4} \frac{L^2}{H} A|A|. \qquad (5)$$

In this predictor the wavelength L determines the length scale and the tidal frequency $\sigma = 1.41 \cdot 10^{-4}$ [s^{-1}] determines the timescale. To allow the migration rate to be expressed in *m/y* while keeping the tuning parameter dimensionless, n is the number of seconds in a year. Since we only have data from areas with a semidiurnal tide, the correctness of this timescale cannot be confirmed. However, this choice is justified by the fact that the net migration is the result of the sediment transport averaged over a tidal cycle. Figure 10 shows that the quality of the predictor is high. The correlation between the predicted and the observed values is 99%. The root-mean-square error is 0.34 m/y.

[26] Three additional data sets have been used to validate the results. Figure 10 shows that the migration predictor estimated the sandwave migration in these three areas very well. As these areas are from distinct other areas than the 9 calibration areas, this suggests that the migration predictor is valid for the whole Southern Bight of the North Sea.

6. Accuracy of the Analysis

[27] To analyze the quality of our analysis, we analyze the accuracy of the data, and the consequences for our approach. These accuracies strongly depend on the measuring procedures, the equipment and the conditions during the surveys. Therefore we are unable to determine the precise accuracies of all data sets. We will give rough estimates of the accuracies based on the available information and on a general evaluation. The bathymetric data contains a number of error sources, positioning errors, depth distortion due to tides and waves and bed level noise due to seasonal variation and small-scale patterns. These sources result in errors when the migration is determined. We analyzed the magnitude and influence of the error sources to determine the accuracy of the migration estimates. The largest obstacle for practical use is the positional error in the bathymetric data. In this section, the influence of the errors is analyzed.

6.1. Measurement Noise

[28] The bathymetric measurements are taken with echo soundings combined with a global positioning system (GPS). Although these systems reach high accuracies, the observations contain errors in the bed level estimates as well as in the observation of the position. Selective availability of the satellite system resulted in a positioning error that reduces from tens of meters in the beginning to about 10 m in the early nineties. Starting around 1998, the positioning error is reduced to about 2 m [*International Hydrographic Organization*, 1998].

[29] In the vertical direction, the water level calculations and the estimate of the speed of sound in the turbulent salt water are the most important sources of errors. The error in the water level calculations can be distinguished, as it is an error that shows up in large parts of data of one survey as global deepening or shallowing, or a strong change in the main slope of the bed. In general, the presence of such an error will lead to a rejection of the survey. The standard deviation of this error is about 20 cm [*Hydrographic Department*, 1990]. The other errors can be assumed to be random noise. For the North Sea, with depths around 30 m, this error has a 25 cm standard deviation [*Hydrographic Department*, 1990].

6.2. Bathymetric Noise

[30] Small-scale bed patterns are another source of inaccuracy in the observations. Superimposed on the sandwaves, smaller-scale ripples and megaripples occur (Table 1). The timescale on which the small patterns evolve is much smaller than both the timescale of the sandwaves and the intervals between the measurement surveys. Therefore the bed level variations of these patterns can be treated as random noise. The standard deviation of this noise depends strongly on the hydrodynamic conditions during and before the survey. However, 10–20 cm is a fair estimate.

[31] On the crests and in the troughs of the sandwaves, megaripples and ripples may result in a horizontal displacement of the highest and deepest point. Given the height of

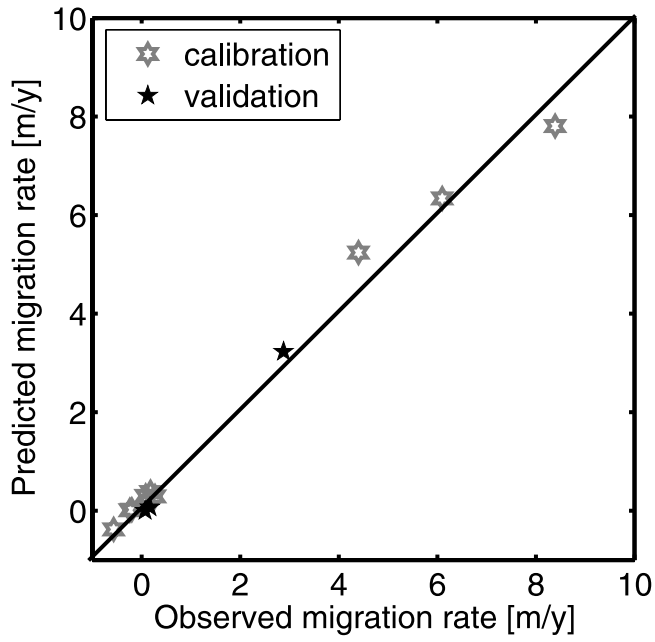

Figure 10. Predicted sandwave migration rates based on the shape characteristics plotted against the observed migration rate. The correlation is high (measure of fitness $R^2 = 0.98$), and the standard deviation is low (0.34 m/y).

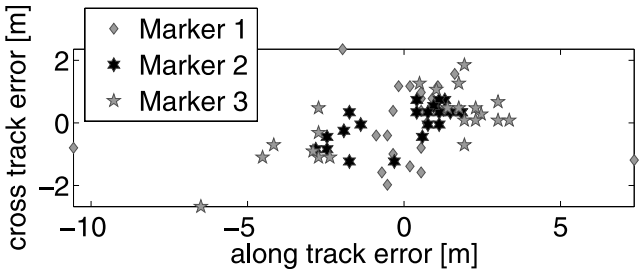

Figure 11. Variation in the observed position of the markers, consisting of concrete-filled tractor tires with a construction for detection. Marker 2 is a steel pyramid, whereas markers 1 and 3 have floating buoys attached.

the patterns and the average slope of the sandwaves (1:50), the standard deviation will be less than 5 m. The error in the troughs are larger than the error on the crests, since the sandwave slopes are gentler in the troughs. We estimate the standard deviation in the trough position at 5 m, and in the crest position at about 2.5 m.

6.3. Positioning Error in the Multibeam Data

[32] In the context of the Delft Cluster project Ecomorphodynamics of the seabed, in which bathymetric, sedimentological and biological data were gathered and compared with each other, three series of high-resolution surveys were taken (September 2001, April 2002, September 2002) on a small part of the Ectomorph area, in which three markers have been placed. In each sessions, surveys were repeated with a 30 minute time interval. The surveys have a 30 cm resolution and show not only sandwaves but also the superimposed megaripples and ripples. Since the migration of the sandwaves within the 1 day sessions is zero, these repeated observations can be used to analyze the positioning errors in the observation.

[33] The three makers can easily be identified as the local maximum in the part of the trough in which they are positioned. Figure 11 shows the positions of the three markers in all surveys. The markers consist of concrete filled tractor tires, with a device mounted on top for detection. Markers 1 and 3 with floating buoys, show a much bigger scatter than marker 2, with the steel frame. Therefore only marker 2 is used, whose position has a bimodal distribution. The first survey session, with fourteen surveys (the cluster of asterisks around (1,0.5) in Figure 11), has a clear offset to the second and third session, 1.8 m and 2.4 m, respectively. Assuming that the heavy markers have not been displaced, this offset can only arise from a positioning error, which is apparently not completely uncorrelated in time.

[34] Next the positions of the sandwave crests are determined using the approach proposed in section 3. Figure 12 shows the mean values and the standard deviation of all displacements of the surveys relative to the first survey. The standard deviation of the observed displacement in the individual surveys of the first session is remarkably smaller (0.5 m), than the standard deviation of the surveys in the other sessions (0.75 m). This is probably related to the small-scale bed forms that are smaller in the first session than in the other sessions.

[35] After the position correction related to the observed marker position, the variation in the mean crest displacement in all three sessions is 0.5 m, which is comparable to the standard deviations for the individual surveys. Almost all crest position estimates are within 1 m from the mean within the session (Figure 12).

6.4. Positioning Error in Data Along the Pipelines

[36] No markers are present in the profiles along the pipeline. Since the pipeline is buried and its position is known only at some locations, it cannot be used for a rectification of the positions. Therefore we have to estimate the accuracy of the crest and trough positions based on other sources. The data set contains two types of error sources.

[37] The first is related to the measurement system, i.e., the single-beam echo sounder and the positioning system. The profiles are measured along the pipeline starting from the oil rigs. This implies a implicit calibration of the positioning system. It can be assumed that the positioning offset between different surveys is no more than a few meters. This assumptions seems to be valid as the position of the pipeline relative to the seabed is determined at several locations along the profiles. However, a solid verification is impossible. The analysis of the system, described in the first part of this section, results in a random positioning error of about 5 m. This is equal to the noise due to small-scale bed forms (section 6.2).

[38] The second error source is the digitization process. As only analogue maps are available for this research, these maps had to be digitized for further analysis. By recurrent digitization of another map, of which the digital data is available, results in a standard deviation of about 10 cm in the vertical. This results in a standard deviation of 1–1.5 m

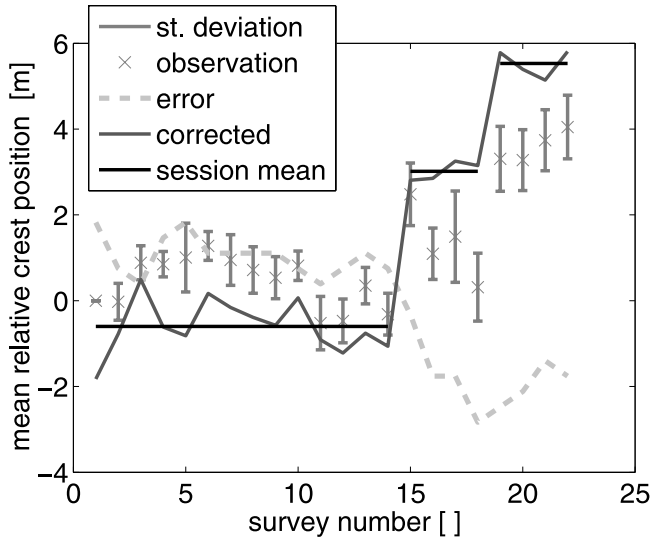

Figure 12. Observed sandwave positions for 22 surveys divided over three 1 day sessions of 14 (September 2001), 4 (April 2002), and 4 surveys (September 2002), relative to the positions of the sandwaves in the first survey. The estimate of the error is based on the observed position of marker 2 relative to its mean position. The data are collected in a part of the Ectomorph area with a high resolution (0.3 m).

for the crests. Owing to the larger small-scale bed patterns in the troughs, the standard deviation in the trough position is almost 2.8 m. Combined, the standard deviation is around 10 m for the crest positions and slightly larger for the trough positions.

7. Discussion of the Approach

[39] The migration predictor is derived by comparing the mean migration in an area with the median characteristics, under the assumption that the sandwaves in the area migrate as a group. However, the predictor formula includes a dependence of the migration rate on the shape characteristics of the sandwaves. This seems to contradict the assumption of group behavior. However, within the areas the variation in the shape characteristics are much smaller than the differences between the areas. The differences between the areas are related to small variations in the hydrodynamic and sedimentary conditions. Most of the variation within the areas are related to bifurcations and other singularities in the patterns. These variation are secondary effects that do not affect the intrinsic uniform structure of the pattern. Consequently, it is possible that the patterns migrate as a group at a speed that depends on the statistics of the shape characteristics and not on the individual characteristics.

[40] For the analysis no information on sediment characteristics, current velocities wave climate etc are required. This might seem a surprise. However, the effect of these conditions is already included in the shape characteristics. The conditions influence the wavelength height and asymmetry of the sandwaves. Since no information of the physical conditions are required, there is no obvious reason why the predictor would not be valid outside the North Sea. The only exception would be the regions in which the tide not semidiurnal. No proof is given yet that the migration rate depends on the tidal frequency, so the model is not valid in regions with a different frequency.

[41] The observation of *Lanckneus and De Moor* [1994] that sandwaves on the Middelkerke sand bank can change their orientation on a seasonal timescale, could be seen as a rejection of our migration predictor. With such a temporal change in asymmetry the predictor could predict migration, where the observations show stationary sandwaves or even migration in the opposite direction. For this reason, it is necessary to be careful to use the predictor in areas with strong seasonal effects, for example near tidal sand banks, since no data has been used from such a domain.

[42] However, there is little evidence that seasonal changes in the asymmetry can be strong enough to corrupt our predictor. In none of the data sets used here, such a change in asymmetry is observed, even in case of multiple surveys per year. Furthermore, *Lanckneus and De Moor* [1994, 1995] give little evidence for a statistically significant change in asymmetry. For the proof of seasonal changes in the asymmetry, *Lanckneus and De Moor* [1994] refer to *Lanckneus and De Moor* [1995]. *Lanckneus and De Moor* [1995, p. 42] state that in the same data sets, ''such reversals, however, do not occur along all reference lines and other lines. . .have characteristic profiles which may temporarily be disturbed by some reversals in asymmetry or by the appearance of an individual large dune.'' This means that the impact on the median asymmetry would be limited. Moreover, in some of the examples of changing asymmetry shown by *Lanckneus and De Moor* [1995], our definition would not give a temporal change in asymmetry of the sandwave where the authors do find a change.

[43] Finally, it can easily be shown that such anomalies can be explained by a combination of the positional error of 10m, the presence of superimposed small-scale megaripples and the existence of bifurcations and crest ends near the transect. In all multibeam data sets, a number of sandwaves can be found with a asymmetry that points opposite to the median asymmetry (see Figure 7). Therefore it is likely that the occurrences of changes in are statistically not very important. Therefore we can assume that our analysis would still hold for the data of *Lanckneus and De Moor* [1994, 1995]. Nevertheless, a comparison with original data from the Middelkerke bank would be a very worthwhile test for the migration predictor.

[44] It is not clear whether bed form migration can be predicted from the shape characteristics of the pattern for every known bed pattern. Bed forms are generally assumed to migrate in the direction of the steeper slope. Moreover, *Carling et al.* [2000] found a relation between the shape and migration rate of river dunes. This points in the direction that a migration predictor could exist for all bed patterns. However, so far no proof of a direct relation between migration rates and the asymmetry has not been given yet.

8. Conclusions

[45] A fast and robust algorithm has been developed to estimate sandwave migration from bathymetric echo sounding data. In a series of surveys, the crest and trough positions and levels are determined. The characteristics of the sandwaves are calculated from these positions and the corresponding bed levels. The changes in the positions in the consecutive surveys give the migration rate. This approach to detect pattern characteristics can be used on both one-dimensional profiles and two-dimensional multibeam maps. Since the approach is independent of flow conditions and scales, it can be used for all types of rhythmic bed patterns in rivers and seas, from ripples to tidal sand banks, as long as the resolution of the data is high enough.

[46] A strong correlation is found between the median shape of the sandwaves and the median migration rate within an area. A single migration predictor based on the shape characteristics reproduces 98% of variability in the migration rates leaving a root-mean-square error of 0.34 m/yr. This is less than the errors in the individual observations of the crest positions, that can be up to 2.5 m. The crest and trough analysis combined with the migration predictor make a useful tool to determine sandwave migration in an area based on a single survey. One has to take care in the regions with tidal sand banks, as the predictor has not been tested yet in such regions with very complex flow patterns.

[47] The observed migration rates vary between 0 and 9 m/yr, which is much lower than the values reported in literature for the North Sea. The migration rates are in the same order of magnitude as the errors in the positioning system. The values reported in literature are strongly affected by these errors. To reduce the effect of these positioning errors

on the estimates of the migration rates, one has to use markers survey over long periods or take many independent surveys.

[48] It is possible to accurately determine sandwave migration from single-beam profiles along pipelines. The mean estimates of the migration rates are quite consistent. This consistency is created by a verification of the positioning system against the known position of the oil rigs. However, the standard deviations are rather high. For each sandwave only one position is given, whereas in multibeam data the positions of each sandwave is estimated several times.

Notation

α constant in migration predictor (y^{-1}).
c sandwave migration rate (my^{-1}).
n number of seconds in a year.
x_{crest} crest position (m).
x_1 trough position south of the crest (m).
x_2 trough position north the crest (m).
z_{crest} crest level (m).
z_1 trough level south of the crest (m).
z_2 trough level north of the crest (m).
A asymmetry.
H sandwave height (m).
L sandwave length (m).
$L1$ lee-slope length (m).
$L2$ stoss-slope length (m).
T typical timescale of bed changes.
σ tidal frequency (s^{-1}).

[49] **Acknowledgments.** Part of the measurements are taken within the Delft Cluster Project Ecomorphodynamics of the Seabed, financed by the Dutch Department of Economic Affairs. The author would like to thank the State Supervision of Mines and the North Sea Directorate of the Netherlands Ministry of transport, Public Works, and Water Management for providing us with the other data sets. The research described in this paper is funded by the Technology Foundation STW, applied science division of NWO, and the technology program of the Ministry of Economic Affairs (project number TWO.5805) and by the EU in the framework of the project HUMOR (contract EVK3-CT-2000-00037).

References

Ashley, G. (1990), Classification of large-scale subaqueous bedforms: A new look at an old problem, *J. Sediment. Petrol.*, *60*, 160–172.

Baptist, M. J. et al. (2001), Eco-morphodynamics of the seafloor, delft cluster, theme 3 coast and river, progress report 2000, technical report, Delft Cluster, Delft, Netherlands.

Besio, G., P. Blondeaux, M. Brocchini, and G. Vittori (2004), On the modelling of sand wave migration, *J. Geophys. Res.*, *109*, C04018, doi:10.1029/2002JC001622.

Carling, P. A., E. Gölz, H. G. Orr, and A. Radecki-Pawlik (2000), The morphodynamics of fluvial sand dunes in the river rhine, near Mainz, Germany. I. Sedimentology and morphology, *Sedimentology*, *47*, 253–278.

Dodd, N., P. Blondeaux, D. Calvete, H. E. De Swart, A. Falques, S. J. M. H. Hulscher, G. Rozynski, and G. Vittori (2003), The use of stability methods for understanding the morphodynamical behaviour of coastal systems, *J. Coastal Res.*, *19*, 849–866.

Hydrographic Department (1990), The assesment of the precision of soundings, *Prof. Pap. 25*, Min. of Defence, London.

Idier, D., A. Ehrhold, and T. Garlan (2002), Morphodynamique d'une dune sous-marine du détropit du pas de calais, *C. R. Geosci.*, *334*, 1079–1085.

International Hydrographic Organization (1998), IHO standards for hydrographic surveys, *Spec. Publ. 44*, Monaco.

Katoh, K., H. Kume, K. Kuroki, and J. Hasegawa (1998), The development of sand waves and the maintenance of navigation channels in the Bisanseto Sea, in *Coastal Engineering 1998: Conference Proceedings*, edited by B. L. Edge, pp. 3490–3502, Am. Soc. of Civ. Eng., Reston, Va.

Knaapen, M. A. F., S. J. M. H. Hulscher, H. J. De Vriend, and A. Stolk (2001), A new type of sea bed waves, *Geophys. Res. Lett.*, *28*, 1323–1326.

Lanckneus, J., and G. De Moor (1994), Environmental setting, morphology and the volumetric evolution of the Middelkerke Bank (southern North Sea), *Mar. Geol.*, *121*, 1–21.

Lanckneus, J., and G. De Moor (1995), Bedforms on the Middelkerke Bank, southern North Sea, *Spec. Publ. Int. Assoc. Sedimentol.*, *23*, 33–51.

McCave, N. (1971), Sand waves in the North Sea off the coast of Holland, *Mar. Geol.*, *10*, 199–225.

Morelissen, R., S. J. M. H. Hulscher, M. A. F. Knaapen, A. A. Németh, and R. Bijker (2003), Mathematical modelling of sand wave migration and the interaction with pipelines, *Coastal Eng.*, *48*, 197–209.

Németh, A. A., S. J. M. H. Hulscher, and H. J. de Vriend (2002), Modelling sand wave migration in shallow shelf seas, *Cont. Shelf Res.*, *22*, 2795–2806.

O'Conner, B. A. (1992), Prediction of seabed sand waves, in *Computer Modelling of Seas and Coastal Regions*, edited by W. Partidge, pp. 322–338, Comput. Mech. Publ., Southampton, U. K.

Otto, L., J. Zimmerman, G. Furnes, M. Mork, R. Soetre, and G. Becker (1990), Review of the physicsal oceanography of the North Sea, *Netherlands J. Sea Res.*, *26*, 161–238.

Reineck, H. E., I. B. Singh, and F. Wunderlich (1971), Einteilung der rippen und anderer mariner sandkrper, *Senckenbergiana Mar.*, *3*, 93–101.

Terwindt, J. H. J. (1971), Sand waves in the Southern Bight of the North Sea, *Mar. Geol.*, *10*, 51–67.

Weber, A., J. van Dalfsen, S. Passchier, A. van der Spek, and S. van Heteren (2004), Eco-morphodynamics of the North Sea seafloor and macrobenthos zonation, in *Marine Sandwave and River Dune Dynamics*, edited by S. Hulscher, T. Garlan, and D. Idier, pp. 308–313, Univ. of Twente, Enschede, Netherlands.

M. A. F. Knaapen, Department of Water Engineering and Management, University of Twente, P.O. Box 217, 7500 AE Enschede, Netherlands. (m.a.f.knaapen@utwente.nl)